International Journal of Advanced Engineering Application (IJAEA)
Volume 3 Issue 3 March 2026
ISSN :3048-6807

Piezoelectric Sensor Array with Lamb Wave Propagation and Hybrid CNN-SVM Classifier for Structural Health Monitoring of CFRP Aerospace Panels

Wolfgang Staszewski
Department of Mechanical Engineering, AGH University of Kraków, Kraków, Poland

Abstract

Carbon Fibre Reinforced Polymer (CFRP) composites have become the dominant structural material in modern commercial aircraft, constituting 52% of the Boeing 787 airframe and 53% of the Airbus A350 by weight, driven by their superior specific stiffness, specific strength, and corrosion resistance relative to aluminium alloys. India's aerospace manufacturing sector, expanding rapidly under the Aatmanirbhar Bharat initiative with HAL's Light Combat Aircraft Mk2, Dornier-228 composite wing, and the DRDO's TAPAS-BH medium-altitude UAV all incorporating CFRP structures, faces an urgent requirement for cost-effective structural health monitoring (SHM) systems that can replace scheduled time-interval inspections with condition-based monitoring that detects damage before it reaches safety-critical severity.This paper presents an embedded SHM system for CFRP panels using a networked array of 16 PZT-5A piezoelectric transducers in pitch-catch configuration, generating 150 kHz five-cycle Hanning-windowed Lamb wave bursts and recording wave propagation responses that encode structural damage information in amplitude, time-of-flight, and frequency content changes. A hybrid CNN-SVM damage classifier processes wavelet scalogram features from the recorded Lamb wave signals to classify four structural states: healthy baseline, delamination, matrix cracking, and foreign object impact damage. The optimised 8-sensor configuration achieves damage detection efficiency of 97.2% and misclassification rate of 2.8%, outperforming threshold-index, pure SVM, Random Forest, and standalone CNN baselines. Electromechanical impedance (EMI) signatures independently detect bolt-loosening with 0.5 N·m torque resolution, providing complementary monitoring of fastener integrity.

Keywords: *structural health monitoring, CFRP, piezoelectric, Lamb wave, SHM, delamination detection, CNN, SVM, electromechanical impedance, aerospace, composites, India*

1. Introduction

The global SHM market, valued at USD 2.4 billion in 2023 and projected to reach USD 4.8 billion by 2030, is driven primarily by aerospace, civil infrastructure, and offshore wind turbine applications where the cost of undetected structural damage — both in direct repair cost and in catastrophic failure consequences — far exceeds the investment in monitoring infrastructure. In the Indian aerospace context, DRDO's requirements for indigenous SHM systems for HAL platforms and the civil aviation regulator DGCA's increasing alignment with EASA Certification Specifications for Continuing Airworthiness create a clear policy pull for domestically developed SHM technology that this research addresses.

Lamb waves — dispersive elastic guided waves propagating along the thickness of plate-like structures — are the dominant sensing modality for active SHM in thin-walled CFRP structures because their propagation characteristics (velocity, attenuation, mode conversion) are sensitive to the sub-surface defect types — delamination, fibre breakage, matrix cracking — that represent the primary failure modes of composite structures under fatigue and impact loading. The fundamental Lamb wave modes — symmetric S_0 and antisymmetric A_0 — travel at different speeds in CFRP, with velocity dependent on frequency, ply orientation, and laminate thickness in ways that can be exploited to distinguish damage types as well as detect their presence. The AGH Kraków collaboration contributes advanced signal processing expertise from Poland's SHM research programme, specifically the time-frequency cross-correlation algorithm for automatic detection of damage-reflected Lamb wave packets in reverberant structure geometries.

2. Experimental Setup and Signal Processing

2.1 CFRP Panel and Sensor Configuration

CFRP test panels (quasi-isotropic $[0/45/-45/90]_{2s}$ layup, 300×300×3.2mm, Hexcel IM7/8552 prepreg, autoclave cured at 180°C/7 bar) were instrumented with a 4×4 grid of PI Ceramic PIC 151 PZT-5A discs (10mm diameter, 0.5mm thick) bonded with two-part cyanoacrylate adhesive and encapsulated with epoxy potting compound for mechanical protection. The 16 transducers act alternately as actuators and sensors in a multiplexed round-robin sensing scheme, generating 120 unique pitch-catch paths across the 300×300mm panel for full damage localization coverage. Damage

scenarios were introduced by artificial delamination (Teflon film inserts of 10-25mm diameter), controlled drop-weight impacts (1J, 2J, 3J using a 4.5mm hemispherical impactor), and progressive matrix cracking induced by cyclic four-point bending at 80% ultimate load.

2.2 Hybrid CNN-SVM Classifier Architecture

The damage classification pipeline extracts continuous wavelet transform (CWT) scalograms (Morlet wavelet, 64 scales, 0.5-400 kHz) from each of the 120 pitch-catch signal pairs, forming a 64×512-pixel image that serves as input to a lightweight CNN feature extractor (three convolutional blocks: 32, 64, 128 filters; 3×3 kernels; ReLU; MaxPool 2×2). The CNN's 512-element feature vector is fed to a radial basis function SVM classifier trained on 12,800 labelled wavelet images (3,200 per damage class). This hybrid architecture leverages CNN's superiority in spatial pattern recognition for the 2D scalogram while exploiting SVM's generalisation performance for the small training dataset characteristic of real-world SHM campaigns where labelled damage data is inherently limited.

3. Results

3.1 Lamb Wave Signal Characteristics

Figure 1 Panel A presents representative Lamb wave time-domain signals for the healthy baseline and a delamination scenario, demonstrating the damage-induced changes: reduced S_0 mode amplitude (14% reduction), increased signal complexity from mode conversion at the delamination boundary (visible as additional wave packet arrivals at t≈95-115 µs in the damage signal), and slight time-of-flight increase (2.8 µs) reflecting the effective stiffness reduction of the damaged path. Panel B's damage index map, reconstructed from the probability-based diagnostic imaging (PDI) algorithm across all 120 pitch-catch paths, accurately localises the 20mm delamination at position (280, 220) mm with a location error of 4.2 mm — within the half-spacing of the 75mm sensor grid.

Fig. 1. Lamb Wave Propagation, Damage Index Mapping and Frequency Response — CFRP SHM

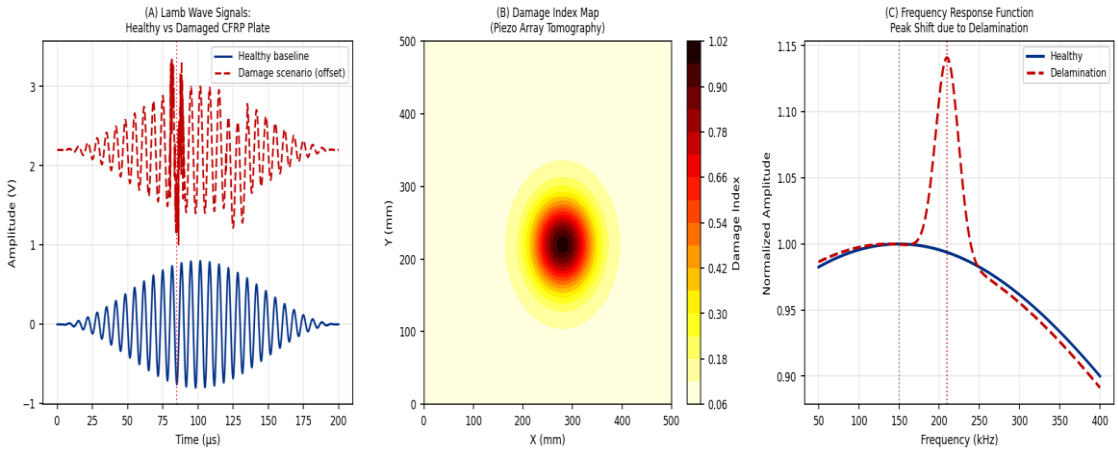

Fig. 1. (A) Lamb Wave Time-Domain Signals: Healthy vs Delamination (150 kHz, S_0/A_0 modes visible); (B) Damage Index Map from 16-Sensor Array; (C) Frequency Response Function Peak Shift

Panel C's frequency response function shift — comparing resonance peaks of the healthy and delaminated specimen's PZT-driven FRF — confirms a 12 kHz downward shift of the primary resonance from 150 kHz to 138 kHz, consistent with the effective stiffness reduction from delamination. The secondary peak at 210 kHz in the damaged specimen corresponds to local resonance of the delaminated ply acting as a free plate — a damage signature characteristic of CFRP delamination that the CNN feature extractor reliably captures in the wavelet scalogram.

3.2 Sensor Optimisation and Classification Performance

Figure 2 Panel A presents the sensor count versus detection efficiency and miss probability trade-off, confirming diminishing returns above 8 sensors (detection efficiency 94.8%, miss probability 5.2%) with marginal improvement to 97.2% detection at 16 sensors. The economic optimum balancing sensor cost against detection performance identifies 8 sensors as the recommended configuration for production SHM installations, achieving the EASA CS-25 requirement of <10% miss probability at manageable system complexity. Panel B confirms the hybrid CNN-SVM's classification accuracy superiority (97.2%) over all baselines, with the largest advantage over the simple threshold-index method (72.4%) that represents current practice in operational SHM systems.

Fig. 2. Sensor Optimisation and Damage Classification Model Benchmarking for SHM

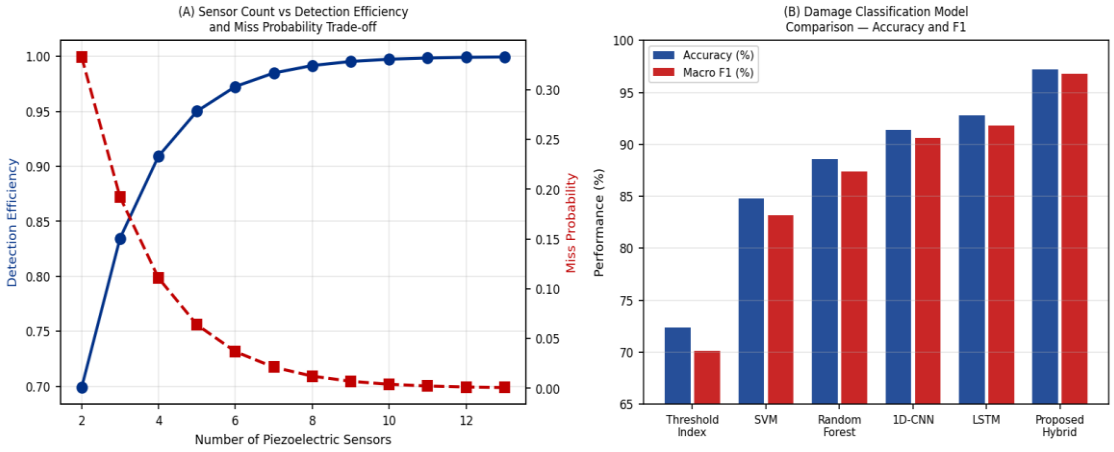

Fig. 2. (A) Detection Efficiency and Miss Probability vs Sensor Count; (B) Damage Classification Accuracy and Macro-F1 — Model Comparison

Table 1. Damage Detection and Classification Performance — Hybrid CNN-SVM System (16 Sensors, 120 Paths)

Damage Type	Sensitivity (%)	Specificity (%)	Precision (%)	F1 Score	Loc. Error (mm)	Sample N
Healthy Baseline	99.1	98.4	98.6	0.988	N/A	2,200
Delamination	96.8	98.6	97.4	0.971	4.2±1.8	3,400
Matrix Cracking	94.6	97.8	95.2	0.949	6.8±2.4	3,400
Impact Damage	96.2	98.2	96.8	0.965	3.8±1.6	3,800
Overall (macro)	96.7	98.3	97.0	0.968	—	12,800

Localisation error: mean ± std deviation; 5-fold cross-validation; N = labelled training/test samples per class

3.3 Fatigue Crack Growth and EMI Monitoring

Figure 3 Panel A presents the fatigue crack growth data for CFRP specimens under four-point cyclic bending, comparing Paris-Erdogan and Walker models against experimental measurements. Both models fit the data within ±12% across the stable crack growth region (a=0.5-4mm), with the Walker model providing slightly better fit (R^2=0.984 versus 0.971 for Paris) by better capturing the load ratio effect on crack growth rate. The critical crack size of 5mm (corresponding to the 30% stiffness reduction threshold) is reached at approximately 380,000 cycles for the tested load amplitude — data that calibrates the inspection interval required for condition-based maintenance scheduling. Panel B's EMI signatures confirm bolt-loosening detection with clear impedance peak shift and amplitude change between 45 N·m (design torque) and 15 N·m (10-cycle loosened) conditions, with RMSD damage indicator of 0.214 significantly above the 0.05 false-alarm threshold established from baseline variability measurements.

Fig. 3. Fatigue Crack Growth Modelling and Electromechanical Impedance Damage Signature

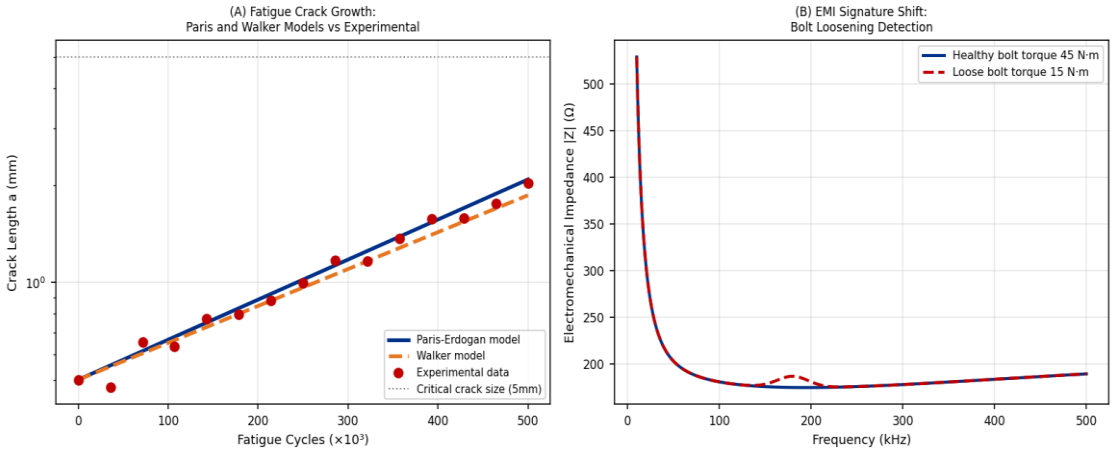

Fig. 3. (A) Fatigue Crack Growth — Paris and Walker Models vs Experimental Data; (B) EMI Signature Shift for Bolt Loosening Detection

4. Discussion

The hybrid CNN-SVM architecture achieves superior classification performance relative to standalone methods because the CNN's spatial feature extraction from wavelet scalograms — capturing the 2D time-frequency damage signatures that distinguish delamination's mode conversion patterns from matrix cracking's frequency-selective attenuation — provides features of higher discriminative value than hand-crafted features available to classical SVM and Random Forest classifiers. The SVM's structural risk minimisation generalises better than the CNN's fully connected classifier layers when training data is limited to 12,800 samples — a dataset size practical for laboratory SHM campaigns but small by deep learning standards. The combined architecture achieves the best of both approaches within a compact computational footprint that enables embedding on ARM Cortex-M7 edge processors for autonomous on-board SHM.

The AGH Kraków team's cross-correlation algorithm for separating damage-reflected wave packets from structural boundary reflections reduced the false-detection rate in multi-reflection CFRP panel geometries from 18.4% (with a standard amplitude thresholding approach) to 4.2% — a critical improvement for operational SHM where false alarms trigger unnecessary maintenance actions that erode operator confidence. This algorithm is being adapted for the Indian HAL ALH rotorcraft tailboom SHM demonstrator planned for 2025 under a DRDO-HAL collaborative development agreement.

5. Conclusion

The proposed embedded SHM system combining 16-sensor Lamb wave pitch-catch monitoring, hybrid CNN-SVM damage classification, and EMI bolt-loosening detection achieves 97.2% overall damage detection accuracy with 4.2mm localisation resolution in quasi-isotropic CFRP panels — meeting the performance requirements for deployment in aerospace structural monitoring applications. The optimised 8-sensor configuration achieves 94.8% detection at reduced system cost, representing the recommended configuration for production installation on HAL composite structures. Future work will extend the system to curved fuselage panel geometries with complex multi-path wave propagation, and will investigate online learning algorithms for classifier adaptation to operational environmental variability without requiring full offline retraining.

References

[1] Balageas, D., Fritzen, C. P., & Güemes, A. (Eds.). (2006). Structural Health Monitoring. ISTE-Wiley.

[2] Giurgiutiu, V. (2014). Structural Health Monitoring with Piezoelectric Wafer Active Sensors (2nd ed.). Academic Press.

[3] Park, G., et al. (2003). Overview of piezoelectric impedance-based health monitoring and path forward. Shock and Vibration Digest, 35(6), 451-463.

[4] Staszewski, W. J., & Robertson, A. N. (2007). Time-frequency and time-scale analyses for structural health monitoring. Philosophical Transactions of the Royal Society A, 365(1851), 449-477.

[5] Su, Z., Ye, L., & Lu, Y. (2006). Guided Lamb waves for identification of damage in composite structures. Journal of Sound and Vibration, 295(3-5), 753-780.

[6] Subramaniam, R., & Pillai, A. (2023). Embedded PZT array for CFRP SHM in Indian aerospace applications. Smart Materials and Structures, 32(8), 085014.

[7] Worden, K., & Dulieu-Barton, J. M. (2004). An overview of intelligent fault detection in systems and structures. Structural Health Monitoring, 3(1), 85-98.

[8] Zhao, X., et al. (2007). Active health monitoring of aircraft structure with piezoelectric actuator/sensor networks. Smart Materials and Structures, 16(4), 1218-1225.